Invisibility of quantum systems to tunneling of matter waves

Sergio Cordero and Gastón García-Calderón*
Instituto de Física, Universidad Nacional Autónoma de México, Apartado Postal 20 364, 01000 México, Distrito Federal, Mexico
(Received 1 July 2008; revised manuscript received 11 March 2009; published 4 May 2009)

We show that an appropriate choice of the potential parameters in one-dimensional quantum systems allows for unity transmission of the tunneling particle at all incident tunneling energies, except at controllable exceedingly small incident energies. The corresponding *dwell time* and the transmission amplitude are indistinguishable from those of a free particle in the unity-transmission regime. This implies the possibility of designing quantum systems that are invisible to tunneling by a passing wave packet.

DOI: 10.1103/PhysRevA.79.052103 PACS number(s): 03.65.Xp, 03.65.Ca, 73.40.Gk

I. INTRODUCTION

The design and construction of one-dimensional artificial quantum structures at nanometric scales has opened a new realm of possibilities on the investigation of fundamental properties of quantum mechanics [1]. One of these properties is tunneling, which represents one of the paradigms of quantum mechanics. As discussed in quantum mechanics textbooks, tunneling of a particle of a given energy through a potential barrier yields in general partial transmission. Full transmission is exhibited in resonant tunneling systems, which at least are formed by two barriers with a well in between. There, unity transmission may be achieved at some specific energies, the so-called resonance energies [2]. This yields, however, a time delay with respect to free propagation that is proportional to the inverse of the resonance energy width [3,4], and hence it allows one to distinguish the tunneling particle from one evolving freely. The issue of total transparency of a tunneling particle by a potential along the full energy range has attracted attention over the years. It has been addressed within different frameworks: inverse scattering theory [5], supersymmetric quantum mechanics [6], Darbox transformation approach [7], and group-theoretical approaches [8]. These works refer to a number of exactly solvable potentials, usually named *reflectionless* or *transparent* potentials, for which the reflection amplitude vanishes identically, while the transmission amplitude has modulus 1 for all incident energies E including the threshold energy value $E=0$. A well-known example is the Pöschl-Teller (P-T) potential well, which for very specific values of the potential parameters attains unity transmission at all energies [9]. However, *transparent* potentials have escaped, to the best of our knowledge, experimental verification and are mainly of interest in mathematically oriented studies. A possible reason is that transparency in these potentials is tightly bound to the functional dependence of the potential.

Here we investigate to what extent one may design potential profiles in one dimension (1D) that, in addition to being totally transparent to a tunneling particle, cannot be detected by interference experiments. Our motivation is purely theoretical and would lead to the possibility of designing *invisible* quantum systems. Our approach rests on analytical properties of the outgoing Green's function of the system in the complex momentum plane that hold provided the potential vanish beyond a distance and the transmission is a coherent, elastic process. These analytical properties consist of having a bound or an antibound pole very close to the energy threshold and all other poles far away and overlapping among themselves.

We find that one may design potential profiles in 1D that possess two regimes for transmission of incident monochromatic energy particles. In one regime, occurring at very small controllable energies close to the energy threshold, i.e., a very small fraction of the potential barrier height, the transmission coefficient rises sharply from zero to unity, and in the other regime, which involves the rest of tunneling energies and energies extending up to several times the potential barrier height, the particle attains essentially unity transmission. We show that in the unity-transmission regime the transmission phase has a vanishing value, which implies indeed that interference experiments cannot detect the scattering potential and, in addition, that the *dwell time*, which provides the relevant time scale for the tunneling process, is indistinguishable from that of a free particle. As a consequence of the above considerations we find that in the unity-transmission regime these systems are indeed invisible to a tunneling particle. Moreover, since in time domain, extremely small energies correspond to very long times, we obtain that these systems are essentially invisible to tunneling by an incident pulse or wave packet. We shall refer to these systems as *invisible* systems.

It is worth noticing that here invisibility refers to a different process from studies that involve the design of a cloak surrounding a system that then becomes invisible to light [10] or with approaches in the quantum domain, refer to as quantum cloaking, where a system is surrounded by a cloak to become invisible to matter waves at certain incident energies in two dimensions (2D) and three dimensions (3D) [11,12]. These approaches are based on ideas from transformation optics and refer only to a time-independent description. We do not surround a system with a cloak but rather we design systems that become invisible to matter waves and consider both the energy and time domains.

Contrary to *transparent* potentials where full transmission is tightly bound to the functional dependence of these potentials, the potentials considered here are robust against some variation in the functional dependence of the potential profile. One may consider rectangular or continuous shapes

*Corresponding author. gaston@fisica.unam.mx

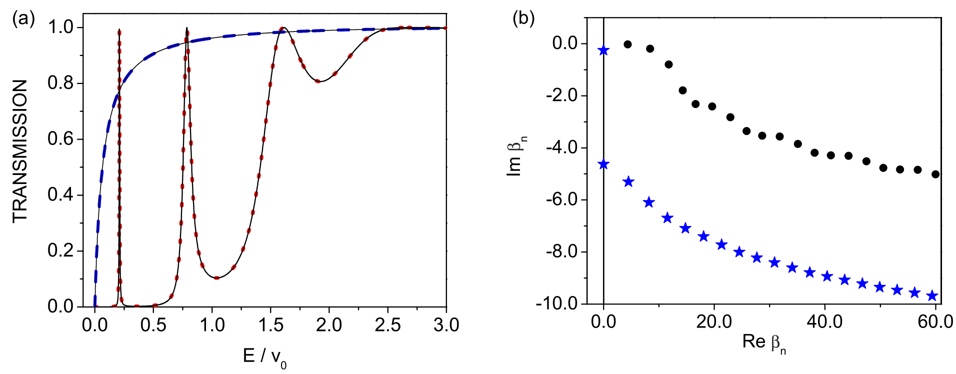

FIG. 1. (Color online) (a) Transmission coefficient as a function of the energy in units of the potential height V_0 for two double-barrier systems. The exact numerical calculation (solid line) is reproduced exactly by Eq. (2) using $N=500$ poles. Both systems have the same barrier height, $V_0=0.2$ eV, and no well depth, $U_0=0$; their well widths are twice the barrier widths, i.e., $w=2b$. One of them (dotted line) has $b=4.0$ nm and exhibits two well-defined resonances along the tunneling region, whereas the other (dashed line), $b=0.4$ nm, shows no resonance structure at all. (b) Distribution of several complex poles of the transmission amplitude in the $\beta \equiv kL$ plane for the potentials in (a): for $b=4.0$ nm (circles) and for $b=0.4$ nm (stars). One sees that by diminishing the values of b, and hence of w, one goes from a system with sharp resonances (poles very close to the real axis) to one with no resonances at all (all poles far away from the real axis). See text.

formed by distinct combinations of barriers and wells.

This work is organized as follows. In Sec. II we consider the resonance formalism and the relationship between the transmission amplitude and the distribution of its complex poles. Section III deals with invisible systems through a number of subsections that discuss, respectively, the rectangular barrier and the Pöschl-Teller potential, multibarrier systems, the dwell time, and wave-packet scattering. Finally, Sec. IV gives the concluding remarks.

II. TRANSMISSION AMPLITUDE AND COMPLEX POLES

Let us consider a particle of mass m and energy E impinging, from $x<0$, on a quantum structure characterized by a potential profile $V(x)$ of length L, i.e., $V(x)=0$ outside the region $0<x<L$. As is well known, the solution to the Schrödinger equation of the problem may be written for $x \leq 0$ as $\psi_<(x,t)=\exp(ikx)+\mathbf{r}(k)\exp(-ikx)$, and for $x \geq L$ as $\psi_>(x,t)=\mathbf{t}(k)\exp(ikx)$, where $\mathbf{r}(k)$ and $\mathbf{t}(k)$ stand, respectively, for the reflection and transmission amplitudes. It is convenient to write the transmission amplitude $\mathbf{t}(k)$ in terms of the outgoing Green's function of the problem, $G^+(x,x';k)$ [13], namely,

$$\mathbf{t}(k) = 2ikG^+(0,L;k)e^{-ikL}, \tag{1}$$

where $k=[2mE]^{1/2}/\hbar$. The reason is that this allows one to obtain a representation for the transmission amplitude as an expansion involving the poles and residues of the outgoing Green's function to the problem. This procedure is in fact numerically equivalent to standard numerical calculations such as the transfer-matrix method [1]. However, it yields a deeper physical insight by establishing a link between the analytical properties of the outgoing Green's function on the complex k plane and the behavior with energy of the transmission phase and the transmission coefficient.

It is well known that the function $G^+(x,x';k)$, and hence the transmission amplitude $\mathbf{t}(k)$, possesses an infinite number of complex poles k_n, in general simple, distributed on the complex k plane in a well-known manner [3,4]. Purely positive and negative imaginary poles $k_n \equiv i\gamma_n$ correspond, respectively, to bound and antibound (virtual) states, whereas complex poles are distributed along the lower half of the k plane. They may be calculated by using iterative techniques as the Newton-Raphson method [14]. The outgoing Green's function $G^+(0,L;k)$ may be expanded as an infinite sum in terms of its poles [13,15]. We have found recently that the expansion of $G^+(0,L;k)\exp(-ikL)$ has better convergence properties. It yields the expansion for the transmission amplitude

$$\mathbf{t}(k) = 2ik \sum_{n=-\infty}^{\infty} \frac{r_n}{k-k_n} e^{-ik_nL}, \tag{2}$$

where r_n follows from the residue of $G^+(x,x';k)$ at the pole k_n [2,13]. The position of the poles k_n on the complex k plane is a function of both the parameters of the potential and the mass of the particle. Consequently, by varying these parameters the poles follow trajectories along the k plane.

For a given combination of rectangular barriers and wells, we denote, respectively, the barrier heights and depths by V_0 and $-U_0$, measured in eV, and the rectangular barrier and well widths by b and w, measured in nm. This is sufficient to characterize a variety of possible combinations of rectangular barriers and wells, as the barrier-well (BW), the barrier-well-barrier (BWB), the well-barrier-well (WBW) systems, and so on. In order to exemplify the above considerations and the relationship of pole distributions with the behavior of the transmission coefficient as a function of energy, which follows from Eq. (2), we consider two double-barrier tunneling systems (BWB) with parameters typical of semiconductor tunneling structures [1], as indicated in Fig. 1. In all calculations the effective electron mass is taken as that of GaAs, i.e., $m=0.067m_e$, with m_e as the free-electron mass. Figure 1(a) provides a plot of the transmission coefficient as a function of energy in units of the potential height, which is the same for both systems. In both systems the well depths are zero and the well widths are twice the barrier widths. In system 1 (dotted line), the barrier and well widths are ten times larger than in system 2 (dashed line). One sees that system 1 exhibits two well-defined resonances along the tunneling region, whereas system 2 exhibits no resonances at all. The above behavior of the transmission coefficient reflects itself in the distribution of the complex poles $k_n = \mu_n - i\nu_n$ of the corresponding transmission amplitude, shown in Fig. 1(b). In the case of system 1 (circles), there appear two complex poles very close to the real $\beta \equiv kL$ axis and one may follow well-known arguments to show that each of them yields a Lorentzian or Breit-Wigner analytical expression for the transmission coefficient near resonance energy [16,17]. From the third pole onward the width of the poles increases steadily and one sees that the transmission coefficient eventually approaches unity. In the case of system 2 (stars), the poles are all situated away from the real axis, except for an antibound pole situated no far from the threshold value. We shall see below how important poles near threshold are for invisibility. Notice that since complex poles obey, from time-reversal invariance considerations [16], the relationship $k_{-n} = -k_n^*$, only poles seated on the fourth quadrant of the β plane have been depicted.

III. INVISIBLE SYSTEMS

A. Rectangular barrier and Pöschl-Teller potentials

Recently it has been shown that total transparency of a very thin single-barrier rectangular potential at all except very small energies follows from a distribution of poles that consists of an antibound pole seated very close to $k=0$ and all other complex poles away from the real k axis and overlapping with each other [18]. The antibound pole k_a may written as [18]

$$\gamma_a \approx -\frac{[mV_0]L}{\hbar^2}. \tag{3}$$

A similar situation holds for the P-T barrier potential $W(x) = V_0/\cosh^2(x/d)$ [9]. Here, we may also denote, respectively, the corresponding barrier height or depth by V_0 or $-U_0$ and the barrier or well widths by the parameters d_b or d_w. The transmission amplitude for the P-T barrier potential reads

$$\mathbf{t}(k) = \frac{\sinh(\pi kd)e^{i\phi}}{\sinh(\pi kd) + i\cos[(\pi/2)\sqrt{1-\eta}]}, \tag{4}$$

with ϕ as a phase and $\eta = 8mU_0d^2/\hbar^2$. Equation (4) has poles at the zeros of its denominator. For $\eta \ll 1$, the P-T potential has an antibound pole very close to $k=0$, namely, at

$$\gamma_a \approx -\frac{[2mV_0]d}{\hbar^2}, \tag{5}$$

which resembles that for the thin rectangular barrier potential written above. Clearly for a P-T well, where the potential parameter is negative, i.e., $-U_0$, a similar relationship holds for a bound state γ_b. The above analytical behavior is different from the well-known total transparency of a single P-T well at all energies, including $E=0$, which occurs for $1+\eta = (2n+1)^2$, with $n=0,1,2,\ldots$ [9]. In this case η may be quite large and the corresponding outgoing Green's function has, as only singularity, a pole at $k=0$. The above results for near energy threshold bound or antibound poles suggest to look for a similar behavior in systems formed by different combinations of barriers and wells for either rectangular or P-T potential profiles. In the case of P-T potentials this necessarily introduces a cutoff in the potential tails and hence the analytical properties of the transmission amplitude become analogous to that of rectangular potentials.

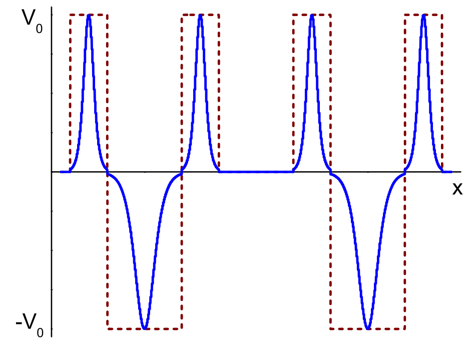

FIG. 2. (Color online) Potential profiles of a two-double-barrier rectangular (2BWB) system (dashed line) and a two-double-barrier P-T potential (dotted line).

B. Multibarrier systems

For both rectangular and continuous potential profiles one may consider different combinations of BWB or WBW systems to form, for example, chains of these systems, as the quadruple-barrier system (2BWB) formed by two BWB systems separated by a distance h, etc. Figure 2 illustrates the potential profiles for a two-double-barrier rectangular potential and a two-double-barrier P-T potential.

Figure 3 provides examples of these pole distributions on

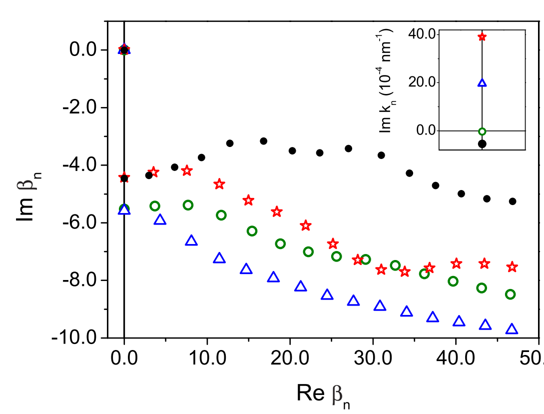

FIG. 3. (Color online) Distribution of the complex poles of the transmission amplitude in the $\beta \equiv kL$ plane for several potential profiles: BWB (triangles), 2BWB (stars), 5BWB (dots), and quadruple-barrier Pöschl-Teller potential (circles). Each potential is characterized by having a bound or an antibound pole very close to the threshold $\beta=0$ (see inset) and all other poles overlapping and away from the real β axis. See text.

the $\beta \equiv kL$ plane, for a number of systems: a BWB (triangles), a quadruple-barrier 2BWB (stars), a ten-barrier 5BWB (dots), and a quadruple-barrier P-T potential (circles). For all the rectangular potential systems, we consider also parameters typical of semiconductor heterostructures: $b=0.4$ nm, $w=0.8$ nm, $h=0.8$ nm, and also $V_0=|U_0|=0.12$ eV, except for the 5BWB system, where the depth of the second and fourth wells is $U=-0.113$ eV. For the P-T potential we choose $V_0=|U_0|=0.12$ eV, $d_b=0.0709$ nm, and $d_w=0.1399$ nm. The effective electron mass is taken also as in the examples considered in Fig. 1, i.e., $m/m_e=0.067$. It is worth noticing that in all examples $\nu_n > \pi/L$, which establishes a scale for the distance from the real k axis of the overlapping complex poles, which fulfill $\mu_{n+1}-\mu_n \sim \pi/L$. The inset shows a zoom of the positions of bound and antibound poles close to $k=0$ for the above systems. The values of bound or antibound poles may be controllable by choosing appropriately the parameters of the potential, as the 5BWB potential exemplifies. Notice that in order to obtain values for the bound or antibound poles so close to the threshold, avoiding extreme values of the barrier widths, it seems necessary that the well depths U_0 differ from zero.

From an analytical point of view the above results for the distribution of the complex poles suggest that the outgoing Green's function in these systems is governed, similarly to the transparent rectangular barrier [18], by the purely imaginary pole seated close to the threshold $k=0$, namely,

$$G^+(0,L;k) \approx \frac{1}{2i(k-i\gamma_q)}e^{ikL}, \tag{6}$$

where $q=a$ or b refers, respectively, to antibound or bound pole and $1/2i$ follows from the residue r_q at the imaginary pole $k_q \equiv i\gamma_q$ [18]. We have verified numerically the validity of the above value of r_q for the distinct systems considered. Substitution of the expression for $G^+(0,L;k)$ given by Eq. (6) into Eq. (2) yields

$$\mathbf{t}(k) \approx \frac{1}{1-i\gamma_q/k}, \tag{7}$$

where we have used $\exp(-ik_qL) \approx 1$. Notice that $k_q \approx 0$ implies that the modulus of $\mathbf{t}$ is very close to unity and that its corresponding phase $\theta \approx \gamma_q/k$ is close to zero except at very small values of k and hence of energy. It is worth noticing that the expression for $G^+(0,L;k)$, given by Eq. (6), exhibits a singularity very close to $k=0$, which resembles the singularity at $k=0$ of the free outgoing Green's function,

$$G_0^+(0,L;k) = \frac{1}{2ik}e^{ikL}. \tag{8}$$

It follows from Eq. (7) that the transmission coefficient reads

$$T(E) = |\mathbf{t}(E)|^2 \approx \frac{1}{1+E_q/E}, \tag{9}$$

where $E_q=(\hbar^2/2m)\gamma_q^2$. Figure 4 exhibits a plot of $T(E)$ as a function of energy in units of the potential height V_0, for several of the systems considered in Fig. 3: 2BWB (dotted) and 5BWB (short-dashed line), for rectangular barrier-well

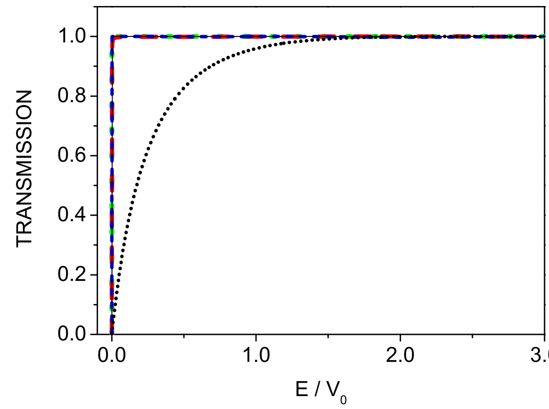

FIG. 4. (Color online) The transmission coefficient $T(E)$ as a function of energy in units of the potential height V_0 is calculated, using Eq. (9), for some of the systems considered in Fig. 3: 2BWB (dotted) and 5BWB (short-dashed line) for rectangular barrier-well potentials and quadruple-barrier P-T potential (dashed line). Also shown is an exact calculation for a quadruple-barrier system (2BSB) with the same parameters as that of 2BWB except that the well depths $U=0$ (short dots). In this case the transmission is not unity along the tunneling region. All calculations are reproduced exactly by numerical calculations of $T(E)$, as exemplified for the 5BWB system (solid line). See text.

potentials and a quadruple-barrier P-T potential (dashed line) as that depicted in Fig. 2. The corresponding values of E_q for the these potentials are, respectively, $E_{2\text{BWB}}=8.68\times10^{-6}$ eV, $E_{5\text{BWB}}=1.67\times10^{-7}$ eV, and $E_{P\text{-}T}=6.19\times10^{-10}$ eV. It might be of interest to compare the above values of E_q, for multibarrier rectangular systems, with that of a single rectangular barrier. This follows by substitution of Eq. (5) into the above expression for E_q to give $E_q=[(2m/\hbar^2)V_0^2/4]L^2$. For example, for a barrier of both, with similar height (i.e., $V_0=0.12$ eV) and effective mass (i.e., $m/m_e=0.067$), a value of $E_q \sim 10^{-6}$ eV would require a width $b=L=0.012$ nm and for $E_q \sim 10^{-8}$ eV, $b=L=0.0012$ nm. The above values for L are extremely small. The widths of barriers and wells in multibarrier systems along the unity-transmission regime are much larger than for a single-barrier system. A similar situation holds regarding P-T potentials.

The calculations using Eq. (9) are indistinguishable from the corresponding exact numerical calculations using the transfer-matrix method [1]. The differences among the distinct systems are only appreciable at very small energies. Figure 4 exhibits also the transmission coefficient for a quadruple-barrier potential with potential depths $U=0$, 2BSB, (short dots). This case is similar to the BSB system (dashed line) presented in Fig. 1. Although it possesses both overlapping complex poles and an antibound pole, the energy of this antibound pole, $E_{2\text{BSB}}=4.18\times10^{-2}$ eV, is not sufficiently close to the energy threshold to exhibit unity transmission along the tunneling region. Notice that it is several orders of magnitude larger than the values for the other systems.

1. Robustness

The phenomenon of invisibility is robust against some variation in the values of the potential parameters of the in-

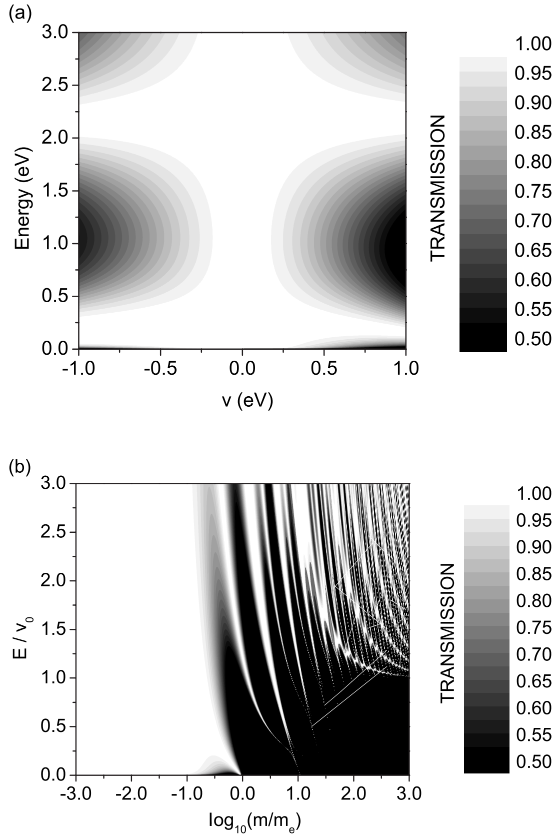

FIG. 5. (a) Transmission contour as a function of the energy E and the parameter $V=V_0=|U|$, for quadruple-barrier systems 2BWB, and all other parameters fixed, for $V>0$, and quadruple-well systems 2WBW, for $V<0$. (b) Transmission contour as a function of the energy E in units of the potential height V_0 for a quadruple-barrier system 2BWB vs $\log_{10}(m/m_e)$, where m is an effective mass and m_e stands for the free-electron mass. See text.

visible system. Within certain limits the variation in effective masses, barrier heights, well depths, barrier widths, and well widths, either for rectangular or continuous shapes as the P-T potentials, keeps the system invisible. To exemplify this, Fig. 5(a) exhibits a contour plot for the transmission coefficient as a function of the energy E and the parameter $V=V_0=|U|$ for rectangular quadruple-barrier systems 2BWB, where all the other potential parameters have the same values as given previously. Notice that for negative values of V the above systems become quadruple-well systems 2WBW. It is also worth noticing that along the "invisibility window," the 2BWB and the 2WBW systems are indistinguishable from each other. The plot for the contour of the transmission coefficient $T(E)$ considers the range of values $0.5 \leq T(E) \leq 1$, which is the range employed for resonance transmission. There is a range of values of V around $V=0$, the free case, that correspond to full transparent systems. One may also consider a similar variation regarding the barrier and well widths, and again within certain limits, full transparency remains robust. Figure 5(b) exhibits the effect of the variation in the effective mass m for the rectangular quadruple-barrier system 2BWB discussed above. This figure displays a contour plot for the transmission coefficient, where $\log_{10}(m/m_e)$ varies in a broad range of values for different incidence energies in units of the barrier height V_0. The value used in the previous calculations, $m/m_e=0.067$, which corresponds to a GaAs quadruple-barrier P-T potential (circles), yields $\log_{10}(0.067)=-1.1739$, which clearly falls within the invisibility regime. The same occurs for $m/m_e=0.1$, where $\log_{10}(0.1)=-1.0$, a value commonly used for GaAsAl barriers. Notice that as the effective mass increases, the system eventually ceases to be invisible and may exhibit a resonance structure.

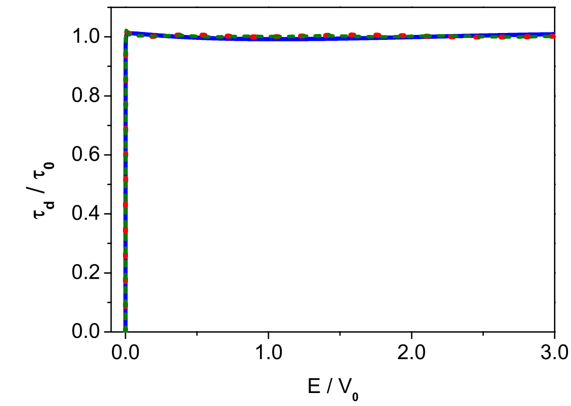

FIG. 6. (Color online) The integral expression for the dwell time τ_d in units of $\tau_0=L/J_0$, as a function of E/V_0, is evaluated numerically for the systems 2BWB (solid line), 5BWB (dotted line), and 10BWB (dashed line). Notice that except at very small energies τ_d is very close to τ_0.

C. Dwell time

Let us now investigate the *dwell time* [19] in these systems. The dwell time is defined as

$$\tau_d(E) = \frac{1}{J_0}\int_0^L |\psi(x,E)|^2 dx, \tag{10}$$

where $J_0=\hbar k/m$ stands for the incoming flux. This quantity measures the amount of time that the incident particle spends within the internal region. One may write it in units of $\tau_0 = L/J_0$, the time it takes to a free particle to traverse the distance L, and express it as [20,21]

$$\frac{\tau_d}{\tau_0} = \frac{1}{L}\int_0^L |\psi(x,E)|^2 dx = T + \frac{1}{L}[T\dot{\theta} + R\dot{\phi}] + \frac{R^{1/2}}{kL}\sin\,\phi, \tag{11}$$

where R stands for the reflection coefficient, $\dot{\theta}$ and $\dot{\phi}$ refer, respectively, to the so-called transmission and reflection times, the dot representing the derivative with respect to k of the phases θ and ϕ of the corresponding transmission and reflection amplitudes $\mathbf{t}(k)$ and $r(k)$. Figure 6 yields a plot of $\tau_d(E)$ in units of τ_0 vs E for several systems: 2BWB (solid line) and 5BWB (dotted line), with parameters as considered above, and 10BWB (dashed line), which is formed by two 5BWB systems separated also by a distance $h=0.8$ nm. The 10BWB system has a length of $L=23.2$ nm and possesses an antibound pole at $-1.091\ 18\times 10^{-3}$ nm^{-1}. The exact numeri-

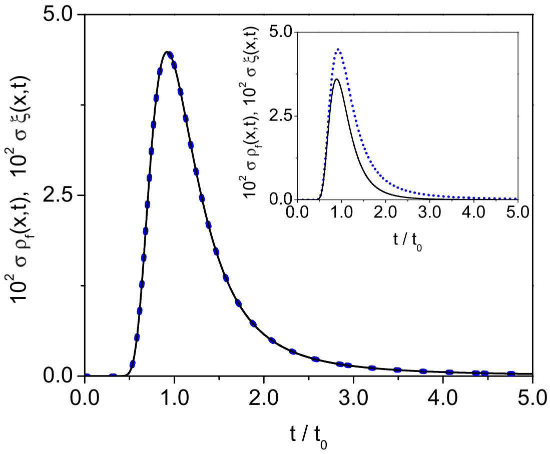

FIG. 7. (Color online) Comparison of two initially identical Gaussian wave packets, one evolving freely (dots), described by $\rho_f(x,t)=|\psi_f(x,t)|^2$, and the other tunneling through a 2BWB system (solid line). Here we calculate $\xi(x,t)=\mathrm{Re}\{\psi_f^*(x,t)\psi(x,t)\}$ $=\cos(\theta)|\psi_f^*(x,t)|^2$ to show that there is no phase dependence on the transmitted phase θ and hence the system is invisible. In contrast, the inset shows that a similar calculation for the 2BSB system considered in Fig. 4, exhibits a phase dependence. The initial parameters of the Gaussian are $\sigma=0.5$ nm and $x_0=-5.0$ nm with an energy $E=0.06$ eV (half the barrier height). The above quantities are calculated at $x=100.0$ nm as a function of time in units of $t_0=(x-x_0)/v_0$.

cal calculation of $\tau_d(E)$ is obtained by integrating the probability density along the internal region of the potential using the transfer-matrix method. One sees that in all cases, except at very small energies, $\tau_d(E)$ is very close to $\tau_0(E)$. The above result implies that the sum of the last two terms on the right-hand side of Eq. (11) adds to a vanishing contribution, although each term by itself may not be small. One may conclude that in these systems, except at very small energies, the time that the tunneling particle spends along the internal region of the potential is indistinguishable from that of a free evolving particle. These systems might be used to make a comparison of the different definitions for tunneling times, which remains a long-debated and controversial subject [19,22,23].

D. Wave-packet scattering

The above discussion refers to monochromatic waves. Let us now consider the tunneling of a Gaussian wave packet on these systems. The initial wave packet $\psi(x,0)$ is represented by

$$\psi(x,0) = Ae^{-(x-x_0)^2/4\sigma^2}e^{ik_0x} \qquad (12)$$

satisfying the condition $|x_0|/2\sigma > 1$, which guarantees that the tail of the Gaussian wave packet is very small near the interaction region $0 \le x \le L$, and may be solved analytically [24]. We could make a comparison along the transmitted region of a wave packet evolving freely, $|\psi_f(x,t)|^2$, with the wave packet that tunnels through the system, $|\psi(x,t)|^2$. However, even if $|\psi_f(x,t)|^2=|\psi(x,t)|^2$ as a function of time, it is not sufficient to conclude that the system is invisible, since there might exist a dependence on the transmitted phase. Indeed if we write

$$\psi(x,t) = e^{i\theta}\psi_f(x,t), \qquad (13)$$

in order to exhibit a possible phase dependence it is more convenient to compare $|\psi_f(x,t)|^2$ with $\mathrm{Re}\{\psi_f^*(x,t)\psi(x,t)\}$ $=\cos(\theta)|\psi_f^*(x,t)|^2$. Thus if $\cos(\theta)=1$, we may conclude that the system is invisible to the tunneling wave packet beyond any doubt. Figure 7 illustrates that this is indeed the case. It yields a comparison of $\xi(x,t)=\mathrm{Re}\{\psi_f^*(x,t)\psi(x,t)\}$ (solid line) for the system 2BWB discussed above with the corresponding free time evolution wave packet $\rho_f(x,t)=|\psi_f(x,t)|^2$ (dots) as a function of time in units of $t_0=(x-x_0)/v_0$. One sees that both solutions are indistinguishable from each other. The inset exhibits a similar comparison for the system 2BSB, whose only difference with the system 2BWB is that the well depths are zero, and hence it does no exhibit unity transmission along the tunneling region as shown in Fig. 6.

IV. CONCLUDING REMARKS

In summary, we predict the possibility of designing artificial quantum systems in 1D that are invisible to a passing wave packet. Hence the system becomes undetectable by matter waves. Although our examples refer to rectangular and P-T multibarrier systems, they are of a general nature in quantum physics and may also be considered in other artificial systems as ultracold atoms in optical lattices. Our results depend on general analytical properties of the transmission amplitude for coherent processes and may open the way to the design, experimental scrutiny, and applications of these quantum systems.

ACKNOWLEDGMENTS

G.G.-C. acknowledges useful discussions with R. Romo, J. Villavicencio, J. G. Muga, and J. Martorell, and the partial financial support of DGAPA-UNAM Grant No. IN115108.

[1] D. K. Ferry and S. M. Goodnick, *Transport in Nanostructures* (Cambridge University Press, Cambridge, UK, 1997).
[2] G. García-Calderón and R. Peierls, Nucl. Phys. A. **265**, 443 (1976).
[3] J. R. Taylor, *Scattering Theory: The Quantum Theory of Nonrelativistic Collisions* (Dover, New York, 2006).
[4] R. G. Newton, *Scattering Theory of Waves and Particles*, 2nd ed. (Dover, New York, 2002).
[5] P. Kurasov and A. Luger, Lett. Math. Phys. **73**, 109 (2005).
[6] S. P. Maydanyuk, Ann. Phys. (N.Y.) **316**, 440 (2005).
[7] A. A. Stahlhofen, Phys. Rev. A **51**, 934 (1995).
[8] G. A. Kerimov and A. Ventura, J. Math. Phys. **47**, 082108

(2006).
[9] L. D. Landau and L. M. Lifshitz, *Quantum Mechanics: Non-relativistic Theory*, 3rd ed. (Butterworth-Heinemann, Oxford, 1981), paragraph 25.
[10] See, for example, J. B. Pendry, D. Schuring, and D. R. Smith, Science **312**, 1780 (2006); U. Leonhardt, *ibid.* **312**, 1777 (2006); Nat. Photonics **1**, 207 (2007).
[11] S. Zhang, D. A. Genov, C. Sun, and X. Zhang, Phys. Rev. Lett. **100**, 123002 (2008).
[12] A. Greenleaf, Y. Kurylev, M. Lassas, and G. Uhlmann, Phys. Rev. Lett. **101**, 220404 (2008).
[13] G. Garcia-Calderon and A. Rubio, Phys. Rev. A **55**, 3361 (1997).
[14] E. Jüli and D. Mayers, *An Introduction to Numerical Analysis* (Cambridge University Press, Cambridge, England, 2003).
[15] R. M. More, Phys. Rev. A **4**, 1782 (1971).
[16] J. Humblet and L. Rosenfeld, Nucl. Phys. **26**, 529 (1961).
[17] E. Merzbacher, *Quantum Mechanics* (Wiley, New York, 1998).
[18] G. Garcia-Calderon and J. Villavicencio, Phys. Rev. A **71**, 024103 (2005).
[19] R. Landauer and Th. Martin, Rev. Mod. Phys. **66**, 217 (1994).
[20] G. García-Calderón, Solid State Commun. **71**, 237 (1989).
[21] E. H. Hauge, J. P. Falck, and T. A. Fjeldly, Phys. Rev. B **36**, 4203 (1987).
[22] E. H. Hauge and J. A. Stovneng, Rev. Mod. Phys. **61**, 917 (1989).
[23] *Time in Quantum Mechanics*, 2nd ed., edited by G. Muga, R. Sala Mayato, and I. Egusquiza, Lecture Notes in Physics Vol. 734 (Springer, Berlin, 2008).
[24] J. Villavicencio, R. Romo, and E. Cruz, Phys. Rev. A **75**, 012111 (2007).